



Synthesis, X-ray structural analysis, antibacterial and DNA-binding studies of a lanthanum bis-(5,5'-dimethyl-2,2'-bipyridine) complex

T. Kondori¹ · N. Akbarzadeh-T¹ · C. Graiff²

Received: 5 September 2018 / Accepted: 25 March 2019 / Published online: 2 April 2019
© Iranian Chemical Society 2019

Abstract

A new complex with the formula $[\text{La}(\text{5,5}'\text{-dmbpy})_2(\text{NO}_3)_3]$ (**a**) [where (5,5'-dmbpy = 5,5'-dimethyl-2,2'-bipyridine)] has been synthesized. The compound was characterized by cyclic voltammetry, elemental analysis and spectroscopic methods (IR, UV–Vis, ¹H-NMR). Single crystals adapted for X-ray diffraction analysis were recorded by slow crystallization from a methanol solution. The complex is neutral being the lanthanum cation chelated by two bipyridine derivative neutral ligands and three bidentate nitrate groups. Electronic spectra show the transition of both ligand field and charge transfer bands. The fluorescence properties of the compound have been studied. The interactions of complex with FS-DNA (salmon sperm DNA) have been studied using UV–Vis, fluorescence spectroscopies and gel electrophoresis. The above-mentioned techniques were used in physiological buffer having pH 7.2. The binding constant (K_b) for interaction in (**a**) with DNA was obtained using UV–Vis spectroscopies ($K_b = 1.2 \times 10^5$) and fluorescence spectroscopies ($K_b = 1.50 \times 10^5$). The binding constant (K_b), the number of binding sites for each 1000 nucleotides (n) and the apparent bio molecular quenching constant (k_q) for FS-DNA were obtained through Stern–Volmer equation. Thermodynamic parameters data (ΔH° , ΔS° and ΔG°) showed that hydrogen bonding and van der Waals interactions have an important function in the interaction of DNA–La(III) complex, and the binding mode is the groove binding. The DNA binding of La(III) complex is spontaneous as suggested by the negative ΔG° . Moreover, the DNA cleavage has been studied using agarose gel electrophoresis. The antibacterial effects of complex (**a**) have also been examined in vitro against standard bacterial strains.

Keywords Single crystals · Fluorescence · FS-DNA · Stern–Volmer equation · Gel electrophoresis · Antibacterial

Introduction

Compounds containing 2,2'-bipyridine molecules are well known in the chemistry literature [1]. Ligand 2,2'-bipyridine contains an extended conjugation system. Bipyridine derivative ligands, such as 5,5'-dmbpy, show good binding ability toward many metals, due to their π -accepting property and strong chelation effect [2–5]. Complexes containing bipyridine derivative ligands have shown various applications in the field of chemistry such as catalysis, luminescent sensors, electron transfer in transition metal complexes and

biological systems, artificial photosynthesis, electrochemistry and organic light-emitting diodes [6–9]. Lanthanide ions and their complexes are used in bioinorganic chemistry due to their properties such as spectroscopic, biological, pharmaceutical, antibacterial and antitumor activity and DNA-binding affinity [10–13]. The functional properties of the lanthanum atom, in general, are strongly affected by factors of the powder, such as purity, chemical composition, particle size and morphology [14]. The binding of small molecules to macromolecules has been a subject actively investigated at the interface of biological chemistry. The interaction of metal complex to DNA may cause DNA damage in cancer cells, prevent the division of cancer cells and finally result to cell death. Thus, DNA-binding studies have an important role in making more effective antitumor factors, and their effectiveness appertains to the binding mode. DNA has number of sites for various non-covalent and covalent interactions with the metal complexes and antitumor drugs. Covalent interactions comprise the coordination of the

✉ N. Akbarzadeh-T
n.akbarzadeh@chem.usb.ac.ir

¹ Department of Chemistry, University of Sistan and Baluchestan, P.O. Box 98135-674, Zahedan, Iran

² Department of Chemistry, Life Sciences and Environmental Sustainability, University of Parma, Parco Area delle Scienze 17/A, 43124 Parma, Italy

nitrogenous base of DNA to the metal ion, whereas small molecules and metal complexes usually bind to DNA in a non-covalent method, which can be classified into three modes: (1) intercalative binding; (2) groove binding; and (3) electrostatic binding [15, 16].

In view of the above attention, we describe herein (1) the synthesis and characterization of a new La(III) complex of 5,5'-dimethyl-2,2'-bipyridine of formula $[\text{La}(5,5'\text{-dmbpy})_2(\text{NO}_3)_3]$; (2) the solid-state structure of the complex by single-crystal X-ray crystallography; (3) the binding mode and propensity of the La(III) complex to FS-DNA using different experimental methods including electronic absorption and fluorescence spectroscopic methods and gel electrophoresis mobility shift assay; (4) the fluorescence quenching mechanism of the metal complex by FS-DNA as well as its interaction forces toward FS-DNA via examining the fluorescence quenching titration at three different temperatures (293, 298 and 303 K) and calculating the thermodynamic parameters (ΔG° , ΔH° and ΔS°); (5) further clarification of the La(III) complex–FS-DNA-binding mode which carried out by examining the effect of iodide ion and salt concentration on fluorescence of the metal complex–DNA system; and (6) the evaluation of the antibacterial effects of the metal complex against a gram-negative (*Escherichia coli*; *E. coli* ATCC 25922) and a gram-positive (*Staphylococcus aureus*; *S. aureus* ATCC 25923) standard strain bacteria examining by standard methods and compared with free ligand (5,5'-dmbpy), metal salt $\text{La}(\text{NO}_3)_3 \cdot 6\text{H}_2\text{O}$ and ceftazolin as a standard antibacterial agent.

Experimental

Materials and instruments

The chemicals and solvents were obtained from Merck. Infrared spectra ($250\text{--}4000\text{ cm}^{-1}$) of solid compounds were obtained as 1% dispersions in CsBr pellets with of a Shimadzu-470 Plus spectrometer. Electronic absorption spectra in DMF solution were obtained using Cary Bio 300 spectrometer with a Heraeus CHN Rapid analyzer. Cyclic voltammograms were recorded using a SAMA500. The $^1\text{H-NMR}$ spectra was recorded at room temperature (298 K) with a Bruker 300 Ultra shield spectrometer. The fluorescence of the complex was performed on a Varian Cary Eclipse fluorescence spectrophotometer. FS-DNA was bought from Sigma Chemical Company. Tris buffer solution is prepared by using distilled water. The fluorescence spectra were measured by a PerkinElmer, LS-45.

Crystallographic data collection and structure determination

X-ray diffraction data for complex (a) were collected at 173 K on a Bruker Apex II single-crystal diffractometer, working with Mo–K α graphite monochromatic radiator ($k_\alpha = 0.71073\text{ \AA}$) and equipped with an area detector. The raw frame data (20 s per frame scan time for a sphere of diffraction data) were processed using SAINT software, and a correction for absorption was made using the SCALE program implemented in the SAINT package to yield the reflection data file. The structure of compound (a) was solved by direct methods with SHELXS-97 and refined against F^2 with SHELXL-2014/7 using anisotropic thermal parameters for all non-hydrogen atoms [17, 18]. The hydrogen atoms were placed in the ideal geometrical positions. Details for the X-ray data collections are reported in Table 1. Crystallographic data for all the compounds have been deposited with the Cambridge Crystallographic Data Centre as supplementary publication (CCDC numbers in Table 1). Copies of the data can be obtained free of charge on application to the CCDC, 12 Union Road, Cambridge CB2 1EZ, UK (fax (+44) 1223 336033; e-mail deposit@ccdc.cam.ac.uk).

Table 1 Main crystallographic parameters for compound (a)

Compound	(a)
Formula	$\text{C}_{24}\text{H}_{24}\text{LaN}_7\text{O}_9$
Molecular weight	693.41
Crystal system	Orthorhombic
Space group	<i>Pbcn</i>
a [Å]	16.8364(12)
b [Å]	9.5128(7)
c [Å]	17.2975(13)
V [Å ³]	2770.4(4)
Z	4
D_{calc} [g cm ⁻³]	1.662
$F(000)$	1384.0
Reflections collected	43,932
Independent reflections	4632
Reflections in refinement	3527
R (int)	0.0214
Refined parameters	187
R_1 [$I > 2\sigma(I)$]	$R_1 = 0.0227$ $wR_2 = 0.0536$
wR_2 [all data]	$R_1 = 0.0341$ $wR_2 = 0.0588$
GOF	1.023
CCDC	1818064

$$R_1 = \Sigma|F_o - F_c|/\Sigma(F_o); wR_2 = [\Sigma[w(F_o - F_c)^2]/\Sigma[w(F_o)^2]]^{1/2}$$

DNA-binding experiments

The stock solutions of FS-DNA were freshly prepared in tris HCl buffer. The experiments containing the interaction of compound (**a**) with FS-DNA were carried out in the buffer including NaCl (50 mM) and tris(hydroxymethyl)-aminomethane, and the experiment was set at pH 7.2 using HCl. FS-DNA concentration was spectrophotometrically specified at 260 nm by an extinction coefficient of $6600 \text{ mol}^{-1} \text{ cm}^{-1}$. This stock solution was kept for 1 week at 277 K. In addition, stock solution of compound (**a**) (10^{-3} M) was prepared in the buffer by heating and stirring. The absorption titration test was performed to study the interaction of the complex (**a**) with FS-DNA by electronic absorption spectroscopy in the UV–Vis region. The stability of the complex (**a**) in aqueous medium was tested by comparing of its UV–Vis spectra at 12-h intervals, and the complex was found to be quite stable. In these tests, a constant concentration of complex (**a**) ($1.0 \times 10^{-5} \text{ M}$) was titrated with raising concentration of FS-DNA. For equilibration, solution of FS-DNA–La(III) complex was incubated for 10 min before spectral records and absorption spectra were obtained after addition of DNA to solution of compound (**a**) in comparison to DNA blank solution. In this study, NaCl was used as a strong electrolyte. The changes in fluorescence emission of La(III) complex–DNA system at room temperature were investigated, while the concentration of NaCl was gradually increased (0.08–0.5 M). After 5-min incubation, the spectrum emission was recorded.

The DNA cleavage experiments with compound (**a**) were conducted to measure the ability of compound (**a**) to retard the motion of FS-DNA in the agarose gel, using incubation of several samples including a fixed amount of FS-DNA ($1.4 \times 10^{-3} \text{ M}$) and various concentrations of complex (**a**) in tris buffer solution, in the absence and presence of an oxidant agent such as hydrogen peroxide. After incubation time (1 h), the samples were mixed with 3 μl of a loading buffer containing methylene blue. Finally, the solution was loaded onto an agarose gel, and the electrophoresis was performed for 20 min at a constant voltage of 120 V. The localization DNA samples on the gel were then stained by adding 6 μl of ethidium bromide solution to the agarose gel solution. For staining, the agarose gel solution was added to EB solution, because painting with little concentrations of ethidium bromide (EB) can specify the localization of DNA within the agarose gel upon irradiation of UV light. The bands were visualized by irradiation with UV light and photographed.

In vitro antibacterial test

The in vitro antimicrobial effects of the complex (**a**) and its ligand were tested against one gram-positive standard strain of *Staphylococcus aureus*, *S. aureus* ATCC 25923,

and one gram-negative standard strain of *Escherichia coli*, *E. coli* ATCC 25922, by using minimum inhibitory concentration (MIC) and minimum bactericidal concentration (MBC) by the broth macrodilution assay in sterile test tubes and the inhibition zone (IZ) by the disk diffusion method. The stock solution of the complex was prepared in distilled water and DMSO. All the inoculated plates were incubated at 310 K for 24 h, and the resulting diameter of each inhibition zone (IZ) presenting no bacterial growth was measured. This inhibitory zone (IZ) assay was performed three times, and results are averaged. Comparison antibacterial effect of complex (**a**) with the cefazolin standard confirmed antibacterial effect.

Synthesis of $[\text{La}(5,5'\text{-dmbpy})_2(\text{NO}_3)_3]$ (**a**)

The mixture of 5,5'-dmbpy (0.065 g, 0.35 mmol) in 10 ml methanol and a solution of $[\text{La}(\text{NO}_3)_3 \cdot 6\text{H}_2\text{O}]$ (0.151 g, 0.35 mmol) in 10 ml methanol were added together. The solution was refluxed under stirring at 586–596 K for 1 week to give milky white crystals; yield: 71.8%, m.p. 553 K. Anal. calc: C, 41.57; H, 3.49; N, 14.14 Found: C, 41.55; H, 3.46, N, 14.03. $^1\text{H-NMR}$ ($\text{DMSO-}d_6$) $\delta = 7\text{--}9$ (12H, bipyridine), 2.85 (12H, 4Me), 2.5 (solvent).

Results and discussion

Synthesis of complex (**a**)

Complex (**a**) was synthesized using the reaction of 0.35 mmol of $[\text{La}(\text{NO}_3)_3 \cdot 6\text{H}_2\text{O}]$ with 0.35 mmol 5,5'-dmbpy in a mixture H_2O and methanol. Suitable crystals of metal compound for X-ray diffraction investigated were prepared using slow evaporation of the colorless solution. An ORTEP sight of complex (**a**) is shown in Fig. 1 together with the atomic labeling system.

Crystalline data of $[\text{La}(5,5'\text{-dmbpy})_2(\text{NO}_3)_3]$ (**a**) are given in Table 1.

Most important bond distances along the angles are reported in Table 2.

The compound is symmetric and it lies on a twofold crystallographic axis. The La–N bond distances are of 2.6622(13) and 2.7033(13) Å and are in agreement with those found in similar compounds [19]. The La–O bond lengths involving nitrate anions are in the range 2.5718(12)–2.5995(13) Å and are in agreement with those found in structures comprising lanthanum atoms coordinated by nitrate anions and reported in the Crystallographic Data Bank. The 5,5'-dimethyl-2,2'-bipyridine ligand is practically planar, and the dihedral angle of $15.31(3)^\circ$ is measured between the mean plane of the ligand and the chelating plane defined by La_1 , N_3 , N_4 atoms. In the crystal packing of the compound, only weak

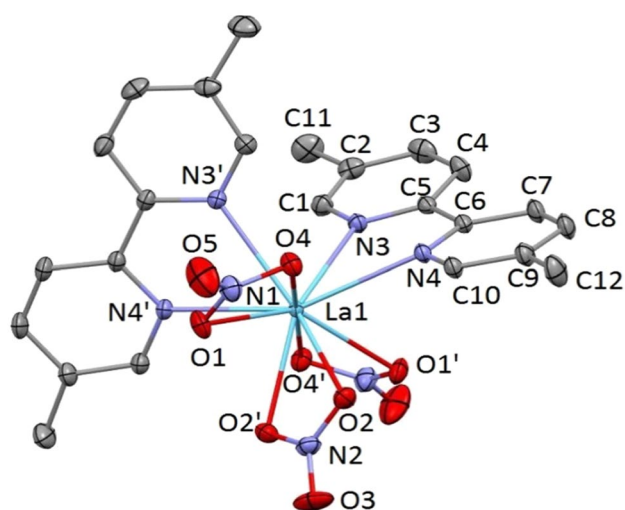


Fig. 1 ORTEP view of compound (**a**). Ellipsoids are drawn at their 30% probability level. Hydrogen atoms are omitted for clarity

Table 2 Selected bond distances (Å) and angles (°) for the complex [La(5,5'-dmbpy)₂(NO₃)₃] (**a**)

Bond	Bond distance	Bond angles	(°)
C1–N3	1.339(2)	O5–N1–O4	121.70(18)
C5–N3	1.349(2)	O5–N1–O1	121.88(17)
C6–N4	1.354(2)	O4–N1–O1	116.42(15)
C10–N4	1.341(2)	O3–N2–O2	121.66(10)
N1–O5	1.215(2)	O3–N2–O2	121.65(11)
N1–O4	1.2667(19)	O2–N2–O2	116.7(2)
N1–O1	1.271(2)	C1–N3–C5	118.49(15)
N2–O3	1.209(3)	C1–N3–La1	118.82(11)
N2–O2	1.2759(18)	C5–N3–La1	121.94(11)
N2–O2	1.2760(18)	C10–N4–C6	118.20(14)
N3–La1	2.6622(13)	C10–N4–La1	120.21(10)
N4–La1	2.7033(13)	C6–N4–La1	119.76(11)
O1–La1	2.5994(13)		
O2–La1	2.5718(12)		
O4–La1	2.5987(15)		

Symmetry code: ' = 1 - x, y, 1/2 - z'

O...H–C interactions between the nitrate anions and the aromatic hydrogen of the 5,5'-dimethyl-2,2'-bipyridine ligand of complex are present [the O...C distances ranging from 3.047(2) to 3.47(3) Å] (Table 3).

IR and UV–Vis investigation [La(5,5'-dmbpy)₂(NO₃)₃] (**a**)

The explanation of the IR spectra of complex (**a**) has been carried out based on the data reported in the literature. In particular, the bands at 835–549 cm⁻¹ are attributed to their

Table 3 Hydrogen bond of [La(5,5'-dmbpy)₂(NO₃)₃] in the crystal packing (Å, °)

D–H...A	D–H	H...A	D...A	D–H...A
C4–H4...O1 ^a	0.9500	2.3600	3.232(2)	153.00
C10–H10...O4	0.9500	2.5300	3.076(2)	117.00
C12–H12A...O5 ^b	0.9800	2.5000	3.473(3)	175.00

Symmetry code for atoms: ^a3/2 - x, -1/2 + y, z; ^b2 - x, 2 - y, -z

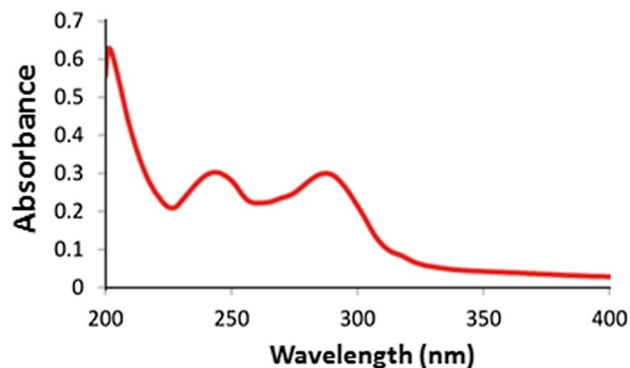


Fig. 2 UV–Vis absorption spectrum of [La(5,5'-dmbpy)₂](NO₃)₃ (**a**)

vibrations bending of C=C=C and C=C=N systems in rings of pyridine [20, 21]. Several strong bands in the range of 1696–1292 cm⁻¹ are associated with the ν(C=N), ν(C=C) stretching [22–25]. The peak at 3196 cm⁻¹ is attributed to the stretching frequency of the ν(C–H) bond in the aromatic region, and the broadband around 3200 cm⁻¹ is associated with the stretching ν(O–H) in H₂O ligand [26, 27]. The peak at 1640 cm⁻¹ is attributed to the vibration stretching of the ν(N–O) [28, 29]. The bands at 1020 cm⁻¹ are assigned to ν(La–O). The band at 472 cm⁻¹ is related to ν(La–N) stretching. The peak at 1256 cm⁻¹ is assigned to the vibration stretching of ν(O–N–O) [30–32].

Electronic spectrum of [La(5,5'-dmbpy)₂(NO₃)₃] (**a**) in DMF solution includes various absorption peaks in the UV region (Fig. 2). Intense UV bands from compound (**a**) in the range 206–250 nm were related to intra-ligand π → π* transition in the free ligand 5,5'-dmbpy [33, 34]. A moderate broadband at 288 nm was attributed to the ligand to metal charge transfer (LMCT) transitions in the complex and has been observed in similar complexes [35].

Electrochemical study of [La(5,5'-dmbpy)₂](NO₃)₃ (**a**)

Cyclic voltammogram (CV) of the compound (**a**) recorded in DMF solution at 298 K is reported in Fig. 3 and is similar to that obtained from other compounds including ligands of

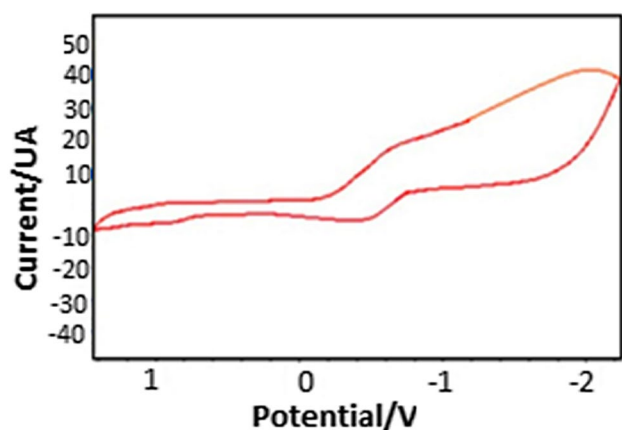


Fig. 3 Cyclic voltammogram for compound $[La(5,5'\text{-dmbpy})_3](NO_3)_3$ (a) in DMF solution at 298 K

bipyridine and phenanthroline [36]. The cyclic voltammogram of complex (a) in DMF solution shows a quasi-reversible reduction wave at -1.93 V which is attributed to the reduction in the 5,5'-dmbpy ligand. The waves at -0.25 V, -0.45 V are assigned to the reduction of lanthanum ions [37, 38].

Luminescent properties of $[La(5,5'\text{-dmbpy})_2](NO_3)_3$ (a)

The fluorescence spectra of 5,5'-dmbpy and compound (a) were recorded at room temperature and in CH_3OH solution (Fig. 4). The free 5,5'-dimethyl-2,2'-bipyridine ligand exhibits a maximum emission band at 340 nm and two shoulder emission peaks at 307 and 395 nm which can be associated with the $\pi^* \rightarrow \pi$ transitions of the ligand [24, 39–41]. Then again, when the compound is illuminated at 285 nm, it exhibits a sharp emission peak at 342 nm and broad emission peaks at 307 and 395 nm. Emission spectra are quite similar, but they are different in emission intensity. Thus,

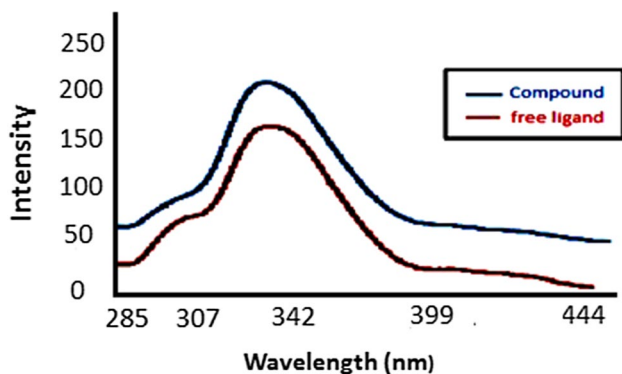


Fig. 4 Fluorescence spectra of free ligand (red) and compound (a) (blue) at room temperature

the enhancement emission band of the compound through complexation is determined to increase rigidity and stability in the structure of the compound and forbid photoinduced electron transfer methods. The synthesized compound can be suggested as a fluorescence substance in the manufacture of optoelectronic device [42, 43].

Study of electronic absorption spectra

Ultraviolet–visible spectroscopy has been largely used to specify binding modes and binding strength of molecules to DNA. The absorption spectrum of DNA alone and the spectrum of complex alone versus the spectrum of DNA and complex when the binding has occurred are shown in Fig. 5.

The UV–Vis spectrum of 5,5'-dmbpy free ligand exhibited two bands at 242 and 285 nm [39]. Comparison with the absorption spectrum of free 5,5'-dmbpy provides evidence that the sharp bands at 255 and 297 nm can be related to the ligand-centered $\pi \rightarrow \pi^*$ transitions of the 5,5'-dmbpy ligands, which are only slightly disturbed by complexation. The experiment confirms that there is an interaction between synthesized compound and FS-DNA [44].

The observed decrease in absorption intensity, called hypochromism, without any change in wavelength (bathochromic and hypsochromic) reveals that the binding mode between synthesized complex and FS-DNA is the groove binding [45, 46]. Finally with further increase in FS-DNA concentration, no changes in the absorption spectra were observed, indicating the saturation of FS-DNA-binding sites (Fig. 6).

In order to investigate the binding ability of metal complex–DNA, the binding constant (K_b) of the complex with FS-DNA can be characterized by plotting of $[DNA]/(\epsilon_a - \epsilon_f) \times 10^{12}$ versus $[DNA] \times 10^6$. The ϵ_a is the extinction coefficient observed for the $A_{obs}/[complex]$ at the given DNA concentration, ϵ_f is the extinction coefficient of the free

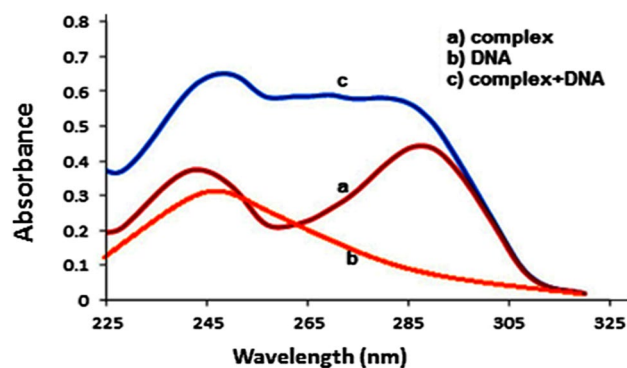


Fig. 5 Absorption spectra of (a) 0.3 ml: 1.0×10^{-5} M complex + 2.7 ml tris HCl buffer, (b) 1.5 ml 1.4×10^{-4} M DNA + 1.5 ml tris HCl buffer, (c) 0.3 ml: 1.0×10^{-5} M complex + 1.5 ml 1.4×10^{-4} M DNA + 1.2 ml tris HCl buffer

Fig. 6 Electronic absorption spectra of metal complex (a) in the absence (curve 1) and presence of increasing amounts of DNA (curve 2–9). [Complex] = 1.0×10^{-5} M, [DNA] $\times 10^{-4}$ M

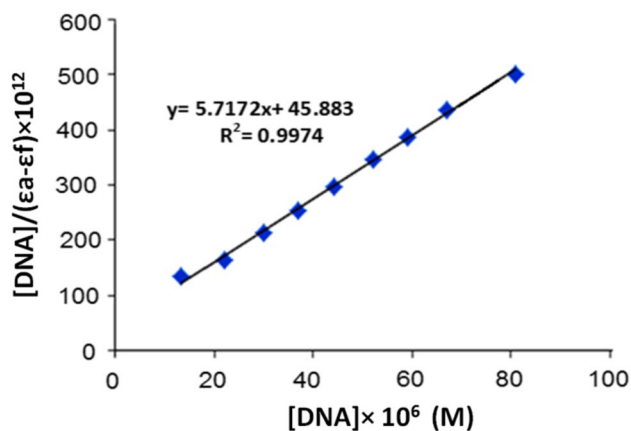
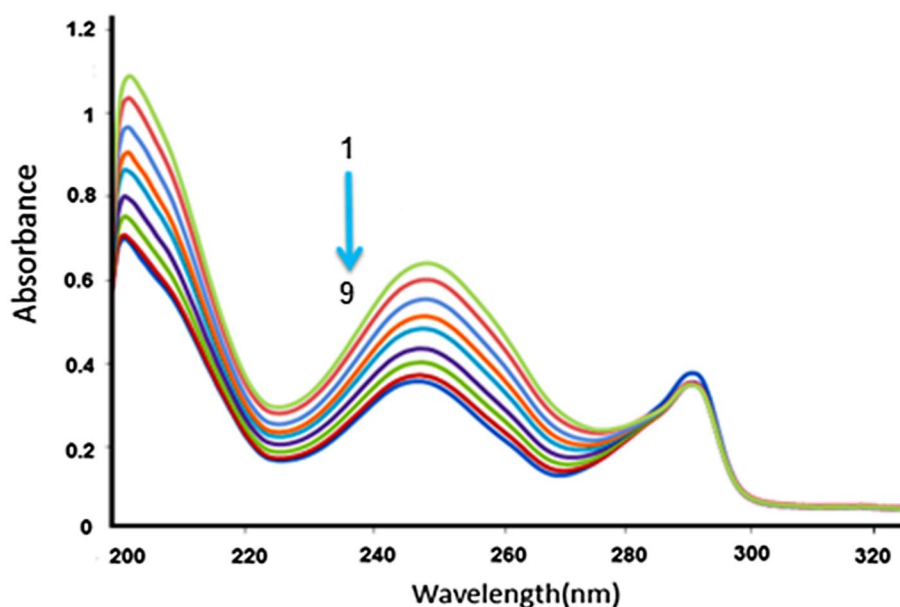


Fig. 7 Plot of $[DNA]/(\epsilon_a - \epsilon_f) \times 10^{12}$ versus $[DNA] \times 10^6$

complex in solution and ϵ_b is the extinction coefficient of the complex when fully bonded to DNA [47]. The binding constant (K_b) was obtained by using the intercept and the slope of the plot of $[DNA]/(\epsilon_a - \epsilon_f) \times 10^{12}$ versus $[DNA] \times 10^6$ Fig. 7.

The high value of K_b ($1.2 \times 10^5 \text{ M}^{-1}$) indicates good interaction between the La(III) compound with FS-DNA and is lower than the value reported for a classical intercalator like ethidium bromide (EB) ($1.4 \times 10^6 \text{ M}^{-1}$) [41, 48–50]. It can be estimated that the binding mode between DNA and compound (a) was not intercalation. In addition, binding with DNA by intercalation causes bathochromism and hypochromism of the absorption because of strong π - π stacking interaction with planar aromatic group of the compound (a) and FS-DNA base pairs [44, 48, 51]. These absorption effect were not observed, in agreement with the structure of

the complex (a) having no planar groups to be as intercalators (Fig. 1).

Study of fluorescence emission

Titration of the metal complex with various amounts of DNA was quantified by measuring quenching which refers to a method that decreases the intensity of fluorescence [52]. This may cause different types of molecular interaction such as energy transfers, excited-state reactions, and the formation of non-fluorescent ground-state metal complex refers to static quenching, whereas collision of the fluorophore–quencher refers to dynamic quenching [53]. The electronic absorption spectroscopy indicates that metal complex efficiently interacts with DNA. It is well found that the interaction of transition metal compound with DNA occurs using covalent and non-covalent interactions [54]. Non-covalent DNA interaction comprises electrostatic, groove and intercalation binding of metal compounds to FS-DNA. The mode of groove binding has been confirmed using presented absorption spectra data [55]. The luminescent properties of complex (a) were studied with excitation at 243 nm at 298 K. The optimum concentration was 10^{-6} M of the metal complex in the solvent of tris buffer. Emission spectra of the complex in the absence and presence of different concentrations of FS-DNA (from 5 to 65 μM) are shown in Fig. 8 (plot of intensity vs wavelength). As observed in this figure, the luminescence of the metal complex with DNA was quenched and the intensity of the emission spectra of the compound with increasing concentrations of DNA decreased, while there was no change in the position and shape of the emission peaks, which confirmed the interaction

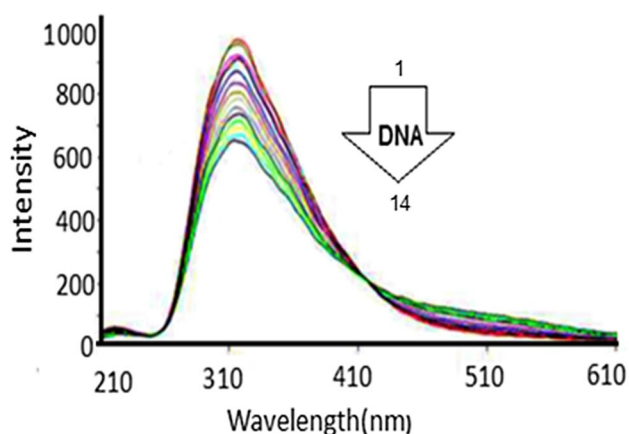


Fig. 8 Fluorescence emission spectra for the La compound, in the absence (curve 1) and presence (curves 2–14) of several concentrations of DNA. The results show that the emission intensity decreases as several concentrations of FS-DNA increase

of metal complex (a)-DNA, and that the interaction binding mode was not intercalation [51, 56].

Stern–Volmer quenching constant

The titration of compound (a) with several concentration of FS-DNA was quantified by measuring the fluorescence quenching of the La(III) complex solution. Generally, we can distinguish between the dynamic and static quenching. The dynamic quenching requires an accidental contact between the quenching compounds and the excited fluorophore. Thus, the rate of quenching depends on viscosity and temperature of the solution. The probability of contact between the quencher and the fluorophore is considerable during the lifetime of the excited species when the quencher concentration is high enough [57]. In the static quenching, the process of quenching performed between the fluorophore in the ground state and the quencher leads to the formation of a stable compound. The kind of quenching can be determined from their different dependence on temperature. The dynamic quenching depends on diffusion, and diffusion coefficients grow with temperature. To clarify the quenching mechanism of La(III) complex by FS-DNA, the equation of Stern–Volmer is applied to analyze the fluorescence quenching data. Following the equation of Stern–Volmer ($F_0/F = 1 + K_{sv} [Q] = 1 + k_q [Q]$), the quenching curve indicates that the quenching of the fluorescence of the complex (a) by using DNA can be explained through the linear Stern–Volmer [58, 59]. In this equation, F_0 is the fluorescence intensity of the complex in the absence of the quencher and F is the fluorescence intensities of the complex in the presence of the quencher, K_{sv} is the Stern–Volmer constant, $[Q]$ is the concentration of quencher (DNA), k_q is the bimolecular quenching constant and τ_0 is the lifetime of

the fluorophore ($\tau_0 = 10^{-8}$ s). The values of K_{sv} were calculated from the slope of the plot F_0/F versus $[DNA]$ at three temperatures (293, 298 and 303 K). The K_{sv} and k_q at several temperatures were calculated. The data are shown in Fig. 9 and Table 4.

In Table 4, the results indicate that the K_{sv} and k_q decrease with the increase in the temperature and k_q is greater than $2.0 \times 10^{10} \text{ l mol}^{-1} \text{ s}^{-1}$ which suggested that the quenching mechanism of metal complex by FS-DNA is a static [60–62].

Number of binding sites (n) and binding constant (K_b)

When a transition metal complex interacts independently with a set of binding sites on a macromolecule such as DNA, the titration data calculated from the fluorescence test can be used to obtain the number of binding sites and the binding constant by equation ($\log (F_0 - F/F) = \log K_b + n \log [Q]$) [55] where n is the number of binding sites and K_b is the binding constant. According to this equation, the values of K_b and n were calculated from the intercept and slope of $\log [(F_0 - F)/F]$ versus $\log [DNA]$ (Fig. 10), respectively. These obtained results (Table 5) demonstrate that K_b decrease with

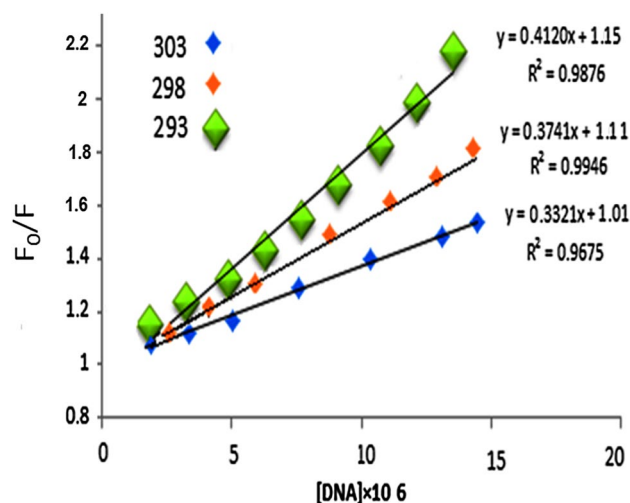


Fig. 9 Stern–Volmer plots of the fluorescence titration of FS-DNA and metal compound (a), at three temperatures (293, 298 and 303 K)

Table 4 Values of K_{sv} and k_q of compound (a) in the interaction and FS-DNA

Complex	T (K)	K_{sv} ($\times 10^5 \text{ M}^{-1}$)	k_q ($\times 10^{13} \text{ s}^{-1} \text{ M}^{-1}$)
(a)	303	3.32	5.35
	298	3.74	6.03
	293	4.12	6.64

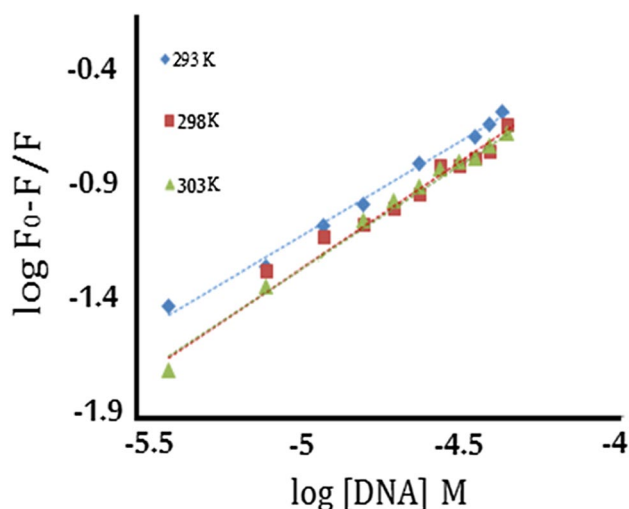


Fig. 10 Log $(F_0 - F)/F$ versus log [DNA]

Table 5 K_b and n values of synthesized complex **1** in the interaction with DNA

Complex	T (K)	K_b (10^5 M^{-1})	n
(a)	303	1.1	0.95
	298	1.5	0.96
	293	2.2	0.98

temperature. The number of binding sites n close to unity means there is one independent group of binding sites on FS-DNA for complex [63].

According to Table 5, the amounts of K_b and n decrease with temperature indicating that the complex formation among FS-DNA and complex (a) may be performed through an exothermic reaction [64]. As a result, the values of K_b are similar to the K_b values obtained from data of electronic absorption ($1.2 \times 10^5 \text{ M}^{-1}$).

Determination of thermodynamic parameters

To better understand the thermodynamics of the reaction between the complex (a) and DNA, the values of entropy change (ΔS°) and enthalpy change (ΔH°) must be specified. The thermodynamic factors explaining binding reactions can be classified into three sections concerning the hydrogen bonding, electrostatic and the hydrophobic interactions with the compounds and FS-DNA-binding sites; the conformational changes in either the nucleic acid or the compound (a) upon binding; and the coupled processes such as changes in the hydration water and ion release. The formation constants between the complex (a) and molecule of DNA at three temperatures (303, 298 and 293 K) were

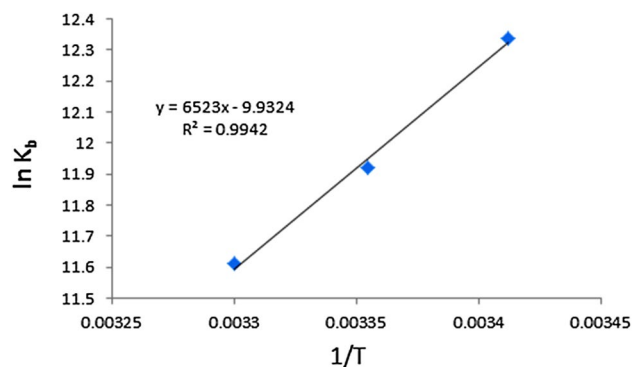


Fig. 11 van 't Hoff plot of compound (a) with FS-DNA at three temperatures (303, 298 and 293 K)

Table 6 Thermodynamic values of complex (a) in FS-DNA interaction

Complex	T (K)	ΔH° (KJ/mol)	ΔS° (J/mol K)	ΔG° (KJ/mol)
(a)	303	-54.23 ± 0.03	-0.082 ± 0.02	-29.38 ± 0.02
	298			-29.79 ± 0.01
	293			-30.21 ± 0.03

calculated. Then, thermodynamic parameters of complex (a)-DNA formation were obtained from the van 't Hoff equation ($\ln K_b = -\Delta H^\circ/RT + \Delta S^\circ/R$) [54]. The parameters ΔS° and ΔH° were calculated by using the plot of $\ln K_b$ versus $1/T$ (Fig. 11). According to these curves, the values of enthalpy change and entropy change were calculated by using the slope ($-\Delta H^\circ/R$) and intercept ($\Delta S^\circ/R$), respectively. Also, the values of ΔG° in the interaction of La(III) complex and FS-DNA can be obtained by the equation of ($\Delta G^\circ = \Delta H^\circ - T\Delta S^\circ = -RT \ln K_b$).

The resulting values of ΔH° , ΔS° and ΔG° are given in Table 6.

As a general rule, intercalation is accompanied with large ΔH° and an unfavorable ΔS° decrease, and the groove binding reactions are mostly performed entropically [56]. The electrostatic interactions indicate values of small or zero ΔH° and positive ΔS° changes, while hydrogen bonding and van der Waals interactions are associated with negative entropy and enthalpy. Thus, the hydrophobic interactions are determined from positive ΔS° and ΔH° changes [65]. According to the thermodynamic data shown in Table 6, the binding forces are spontaneous since the Gibbs free energy change is negative, and enthalpy and entropy changes are negative. This indicates the complex (a) was kept in FS-DNA grooves via hydrogen bonding and van der Waals interaction force. The negative amounts of ΔH° reveal exothermic interaction.

Effects of the ionic strength on interaction

Investigation of the spectral change against various ionic strengths is a technique for suggesting the kind of binding between DNA and complex [51]. The phosphate component of DNA makes it an anionic polyelectrolyte which has been balanced by some cations like K^+ and Na^+ . These cations are concentration dependent, i.e., changing the amount of salts such as NaCl in the medium, and not only the ionic strength is affected, but also the disturbance of the electrostatic interaction between the small molecules and the DNA. The mode of electrostatic is a non-covalent binding, which is served as auxiliary mode to assist intercalation and groove binding. If the binding interaction of electrostatic exhibits an important role in the complex interaction with DNA, the strength of interaction will decrease simultaneously with increasing NaCl concentration in the environment. Thus, any increase in the ionic strength of the medium may prevent the electrostatic interaction [66]. The results of the experiment show that the fluorescence intensity of the La(III) complex with FS-DNA almost did not change with raising the salt concentration (Fig. 12), demonstrating that there was no electrostatic interaction between complex (a) and FS-DNA, which is in agreement with the molecular structure of complex (a) that has no positive charge. Thus, such data showed that the binding of the metal complex and DNA was not electrostatic binding [56, 67].

Iodide quenching method

Study of iodide quenching is a process to investigate the binding mode of fluorescent compounds. If the interaction of compound (a) with DNA is electrostatic or intercalation binding, the fluorescence intensity of the compound and DNA system cannot be quenched through increasing different concentrations of KI [68]. Figure 13 shows the quenching of I^- ions as anionic quencher by complex (a). This figure shows that a small change in iodide quenching

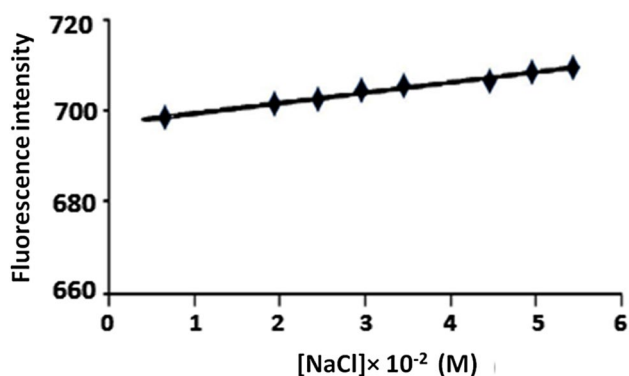


Fig. 12 Plot of fluorescence intensity versus [NaCl]

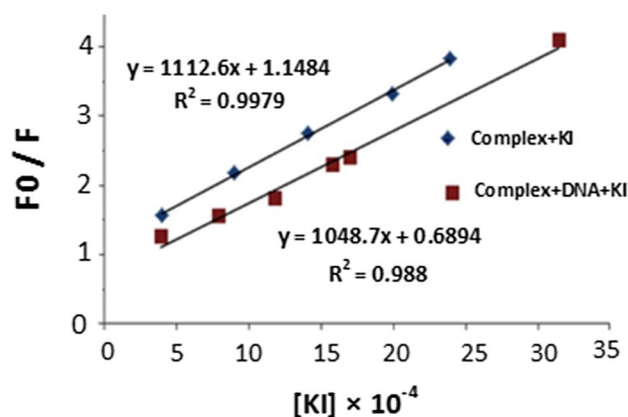


Fig. 13 Stern–Volmer plot of the fluorescence titration results of the compound (a)

interactions can be observed when the complex was bound to FS-DNA, which shows that the binding of complex (a) with DNA was not intercalation mode; therefore, iodide quenching results indicated that groove binding should be the interaction mode of the complex with FS-DNA.

Agarose gel electrophoresis

The gel electrophoresis is a way for investigating mobility of DNA in the environment of agarose gel on the influx of electric potential [68]. In these tests, changes in electrophoretic migration of FS-DNA in the absence and presence of different concentrations of the complex (a) are usually taken as the proof of complex–DNA interaction. Delay in the electrophoretic migration of the FS-DNA band could be assigned to the binding of La(III) complex in different sites on DNA causing raise in its molecular weight, size and shape. Agarose gel electrophoresis patterns for the cleavage of DNA after being treated with the complex of various concentrations are shown in Fig. 14. This electrophoretogram shows that the presence of La(III) complex in DNA samples (lanes 1–6) slows down the migration of FS-DNA by increasing the concentration of La(III) complex which clearly proves the interaction between the two. These results are consistent with other reports [46, 69]. The complex is more effectively capable to cleave FS-DNA in the presence of an oxidant such as H_2O_2 (1–6 in the left) than the absence of that, which this result may be attributed to produce a diffusible hydroxyl free radical. This hydroxyl free radical can be formed by interaction of metal ions with H_2O_2 to produce molecular oxygen or hydroxyl free radical (the Haber–Weiss reaction) that may damage DNA through chemistry and suggest the cleavage of DNA is oxidative and catalytic [56, 70].

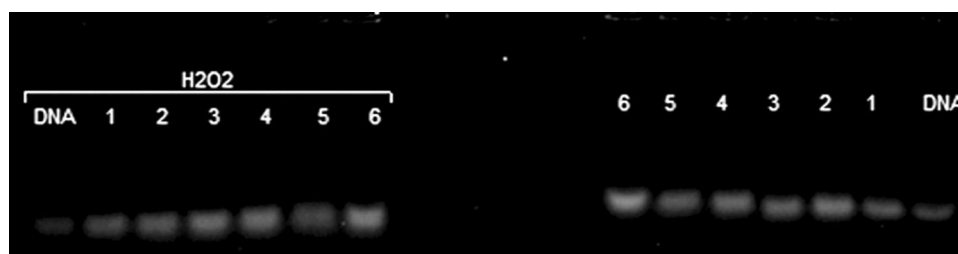


Fig. 14 Gel electrophoresis of FS-DNA (1.4×10^{-3} M) by using various concentrations of complex (**a**) at room temperature: lane DNA: DNA control; lanes 1–6 (in the right): FS-DNA + La(III) complex (1,

1.1, 1.2, 1.3, 1.4, 1.5×10^{-5} M, respectively). Lanes 1–6 (in the left) similar to lanes 1–6 (in the right) but in the presence of H_2O_2

Table 7 MIC, MBC and IZ values of the free ligand and its La(III) complex

Compound	MIC (mg/ml) <i>E. coli</i> , <i>S. aureus</i>	MBC (mg/ml) <i>E. coli</i> , <i>S. aureus</i>	Inhibition zone (mm) <i>E. coli</i> , <i>S. aureus</i>
$La(NO_3)_3 \cdot 6H_2O$	0.003–0.025	0.006–0.025	18–15
Free ligand	0.012–0.012	0.025–0.025	6–6
Complex (a)	0.012–0.006	0.025–0.0125	27–29
Cefazolin	–	–	28

Study of antibacterial properties

Minimum inhibitory concentration (MIC) and minimum bactericidal concentration (MBC) for the ligand and complex were obtained by broth macrodilution method [71]. The inhibition zone (IZ) was obtained by the disk diffusion procedure, using different types of bacterial strains. The solution of 0.5 McFarland standard was taken as a turbidity standard. After reviewing the data, we understand that the complex (**a**) exhibits higher antibacterial properties than ligand of 5,5'-dmbpy. The increased the antibacterial activity of complex (**a**) can be illustrated on the basis of Overtone's concept and Tweedy's chelation theory [72–74]. After chelation, there is a decrease in the polarity of the metal atom, because of the partial sharing of its positive charge with the donor groups and also due to π -electron delocalization on the whole chelate ring. Complex (**a**) prefers interactions with lipids which are important constituents of the cell wall. Also, the decreasing polarity led to an increase in the lipophilic character of the chelates. An interaction between lipids and the complex is successful, which may lead to further breakdown of the cell [75]. The amount of the antibacterial activity for the complex (**a**) was measured using agar well diffusion experiment in a medium of Muller–Hinton agar (MHA) plates. These plates must be incubated at 310 K for 24 h. Finally the resulting diameter of each IZ together with the results of MIC and MBC is indicated in Table 7. At the end, the result exhibited that complex (**a**) is stronger antibacterial

agent than free ligand and metal salt. Furthermore, the antibacterial effects of free ligand (5,5'-dmbpy), the metal salt [$La(NO_3)_3 \cdot 6H_2O$] and cefazolin (a standard confirmed antibacterial effect for *E. coli*) were also measured at the same conditions which enable us to compare them with the newly synthesized La(III) [76].

Conclusion

We reported the preparation of the metal complex (**a**) of formula [$La(5,5'\text{-dmbpy})_2(NO_3)_3$]. The metal complex was characterized by X-ray diffraction technique, FT-IR, UV–Vis spectroscopy, 1H -NMR, cyclic voltammetry and elemental analysis. The photoluminescence properties of the compound and ligand were studied, and a fluorescence intensity increase was observed. The interaction of complex (**a**) with FS-DNA was studied by several methods such as absorption spectroscopy, fluorescence titration spectra and agarose gel electrophoresis. The results obtained are: (1) UV–Vis studies revealed that the complex (**a**) has a good interaction with FS-DNA having a proper value of binding constant; (2) the results of fluorescence studies show quenching of La(III) complex by FS-DNA via a static mechanism and decrease in K_b values with the increase in temperature showing the exothermic interaction; (3) thermodynamic parameters obtained from the fluorescence data indicate that van der Waals and hydrogen bonding play a major role in the interaction between the La(III) complex and FS-DNA; thus, binding mode seems to be groove binding; (4) as change in the ionic strength of the medium does not affect the fluorescence intensity of the La(III) complex–DNA system, the binding mode should not be electrostatic; (5) the effect of iodide anion on the fluorescence intensity of complex La(III) is moderately more than that of the La(III) complex–DNA system. The results suggest that the antibacterial effects of the complex (**a**) are stronger than the free ligand and La(III) salt.

Supplementary material

Supplementary crystallographic data for (a) can be obtained free of charge via <http://www.ccdc.cam.ac.uk/conts/retrieving.html> or from the Cambridge Crystallographic Data Centre, 12 Union Road, Cambridge CB2 1EZ, UK; fax: (+44) 1223 336 033; or e-mail: deposit@ccdc.cam.ac.uk.

Acknowledgements The authors sincerely thank the University of Sistan and Baluchestan for financial support of this work.

References

1. A. Zelewsky, *Inorganic Chemistry, Stereochemistry of Coordination Compounds* (Wiley, New York, 1996)
2. N. Alfi, M. Khorasani-Motlagh, A.R. Rezvani, M. Noroozifar, K. Molčanov, *J. Mol. Struct.* **1137**, 771 (2017)
3. N.R. Kelly, S. Goetz, C.S. Hawes, P.E. Kruger, *Inorg. Chim. Acta* **403**, 102 (2013)
4. V. Amani, N. Safari, B. Notash, *J. Iran. Chem. Soc.* **10**(4), 751 (2013)
5. N.T. Pour, A. Khalighi, M. Yousefi, V. Amani, *Synth. React. Inorg. Met. Nano-Met. Chem.* **45**(9), 1427 (2015)
6. A. Wojciechowska, Z. Staszak, W. Bronowska, A. Pietraszko, M. Cieślak-Golonka, *Inorg. Chem.* **40**(8), 1871 (2001)
7. A. Wojciechowska, Z. Staszak, W. Bronowska, A. Pietraszko, M. Cieślak-Golonka, *J. Mol. Struct.* **654**(1), 197 (2003)
8. A.G. Zavozin, N.I. Simirskaya, Y.V. Nelyubina, S.G. Zlotin, *Tetrahedron* **72**(47), 7552 (2016)
9. F. Havas, N. Leygue, M. Danel, B. Mestre, C. Galaup, C. Picard, *Tetrahedron* **65**(36), 7673 (2009)
10. W.S. Liu, T.Q. Jiao, Y.Z. Li, Q.Z. Liu, M.Y. Tan, H. Wang, L. Wang, *J. Am. Chem. Soc.* **126**(8), 2280 (2004)
11. G. Mancino, A.J. Ferguson, A. Beeby, N.J. Long, T.S. Jones, *J. Am. Chem. Soc.* **127**(2), 524 (2005)
12. L. Pan, K.M. Adams, H.E. Hernandez, X. Wang, C. Zheng, Y. Hattori, K. Kaneko, *J. Am. Chem. Soc.* **125**(10), 3062 (2003)
13. A.Y. Robin, K.M. Fromm, *Coord. Chem. Rev.* **250**(15–16), 2127 (2006)
14. S. Khanjani, A. Morsali, *J. Mol. Liq.* **153**(2), 129 (2010)
15. G. Wang, H. Wang, Y. Ling, Y. Tang, X. Yang, R.C. Fitzmorris, C. Wang, J.Z. Zhang, Y. Li, *Nano Lett.* **13**, 3026 (2011)
16. N. Erlitzki, K. Huang, S. Xhani, A. Farahat, *J. Biol. Chem.* **231**, 95 (2017)
17. G.M. Sheldrick, *SADABS* (Bruker AXS, Madison, 1998)
18. G.M. Sheldrick, *Acta Crystallogr. Sect. A* **64**, 11 (2015)
19. A.R. Al-Karaghoul, J.S. Wood, *Inorg. Chem.* **11**(10), 2293 (1972)
20. V. Amani, N. Safari, H.R. Khavasi, *Polyhedron* **26**(15), 4257 (2007)
21. V. Amani, N. Safari, H.R. Khavasi, P. Mirzaei, *Polyhedron* **26**(17), 4908 (2007)
22. M.S. Gaafar, I. Shaarany, T. Alharbi, *J. Alloys Compd.* **616**, 625 (2014)
23. C.-T. Cao, Y. Bi, C. Cao, *Spectrochim. Acta Part A Mol. Biomol. Spectrosc.* **163**, 96 (2016)
24. V. Amani, R. Alizadeh, H.S. Alavije, S.F. Heydari, M. Abafat, *J. Mol. Struct.* **1142**, 92 (2017)
25. R. Alizadeh, V. Amani, *Struct. Chem.* **22**(5), 1153 (2011)
26. Z.-M. Sun, J.-G. Mao, Y.-Q. Sun, H.-Y. Zeng, A. Clearfield, *Inorg. Chem.* **43**(1), 336 (2004)
27. G.A. Pitsevich, A.E. Malevich, E.N. Lovskaya, I.Y. Doroshenko, V. Sablinskas, V.E. Pogorelov, I.D. Dovga, V. Balevicius, *Vib. Spectrosc.* **79**, 67 (2015)
28. M. Alibrahim, H. Shlewit, *Period. Polytech. Chem. Eng.* **51**(2), 57 (2007)
29. M. Merroun, C. Henning, A. Rossberg, T. Reich, R. Nicolai, K.H. Heise, S. Selenska-Pobell, *Uranium in the Aquatic Environment* (Springer, Berlin, 2002), p. 505
30. S.N. Ostad, S.M. Emadi, S. Tavajohi, V. Amani, A. Abedi, *Bull. Korean Chem. Soc.* **33**, 3891 (2012)
31. F. Shahbazi-Raz, V. Amani, E. Bahojb-Noruzi, N. Safari, *Inorg. Chim. Acta* **435**, 262 (2015)
32. L. Rintoul, A.S. Micallef, S.E. Bottle, *Spectrochim. Acta Part A Mol. Biomol. Spectrosc.* **70**(4), 713 (2008)
33. S.N. Ostad, A. Abedi, V. Amani, P. Karimi, S. Heydarnezhad, *J. Iran. Chem. Soc.* **13**(8), 1417 (2016)
34. H.H. Repich, S.I. Orsyk, V.V. Orsyk, Y.L. Zborovskii, V.I. Pekhnyo, M.V. Vovk, *J. Mol. Struct.* **1144**, 225 (2017)
35. A.R. Rezvani, H. Hadadzadeh, B. Patrick, *Inorg. Chim. Acta* **336**, 125 (2002)
36. M. Shahid, P.K. Sharma, Z.A. Siddiqi, F. Sama, I.A. Ansari, M. Khalid, *J. Mol. Struct.* **1063**, 313 (2014)
37. H. Saravani, M. Khajehali, *Orient. J. Chem.* **31**(4), 2351 (2015)
38. K.M. Raj, B.H.M. Mruthyunjayaswamy, *J. Mol. Struct.* **1074**, 572 (2014)
39. R. Alizadeh, V. Amani, *Inorg. Chim. Acta* **443**, 151 (2016)
40. A. Abedi, E. Saemian, V. Amani, *J. Struct. Chem.* **56**(8), 1545 (2015)
41. G. Hennrich, H. Sonnenschein, U. Resch-Genger, *J. Am. Chem. Soc.* **121**(21), 5073 (1999)
42. Z. Kowser, U. Rayhan, S. Rahman, P.E. Georghiou, T. Yamato, *Tetrahedron* **73**(36), 5418 (2017)
43. N. Chattopadhyay, A. Mallick, S. Sengupta, *J. Photochem. Photobiol. A Chem.* **177**(1), 55 (2006)
44. K. Karami, Z.M. Lighvan, S.A. Barzani, A.Y. Faal, M. Poshteh-Shirani, T. Khayamian, M. Dušek, *New J. Chem.* **39**(11), 8708 (2015)
45. M.S. Deshpande, A.A. Kumbhar, A.S. Kumbhar, M. Kumbhakar, H. Pal, U.B. Sonawane, R.R. Joshi, *Bioconjug. Chem.* **20**(3), 447 (2009)
46. K. Abdi, H. Hadadzadeh, M. Salimi, J. Simpson, A.D. Khalaji, *Polyhedron* **44**(1), 101 (2012)
47. W.A. Wentz, A.S. Danell, *Int. J. Mass Spectrom.* **421**, 124 (2017)
48. U. Chaveerach, A. Meenongwa, Y. Trongpanich, C. Soikum, P. Chaveerach, *Polyhedron* **29**(2), 731 (2010)
49. Y. Zhang, M. Wang, Q. Xie, X. Wen, S. Yao, *Sensors Actuators B Chem.* **105**(2), 454 (2005)
50. L.K. Fraiji, D.M. Hayes, T.C. Werner, *J. Chem. Educ.* **69**(5), 424 (1992)
51. F.-Y. Wu, Y.-L. Xiang, Y.-M. Wu, F.-Y. Xie, *J. Lumin.* **129**(11), 1286 (2009)
52. G. Crivat, J.W. Taraska, *Trends Biotechnol.* **30**(1), 8 (2012)
53. Q.-L. Zhang, J.-G. Liu, H. Chao, G.-Q. Xue, L.-N. Ji, *J. Inorg. Biochem.* **83**(1), 49 (2001)
54. A. Heydari, H. Mansouri-Torshizi, *RSC Adv.* **6**(98), 96121 (2016)
55. A. Belatik, S. Hotchandani, J. Bariyanga, H.A. Tajmir-Riahi, *Eur. J. Med. Chem.* **48**, 114 (2012)
56. Z. Moradi, M. Khorasani-Motlagh, A.R. Rezvani, M. Noroozifar, *J. Biomol. Struct. Dyn.* **36**(3), 779 (2018)
57. S. Kashanian, M.M. Khodaei, P. Pakravan, *DNA Cell Biol.* **29**(10), 639 (2010)
58. S.M. Ahmadi, G. Dehghan, M.A. Hosseinpourfeizi, J.E.N. Dolatabadi, S. Kashanian, *DNA Cell Biol.* **30**(7), 517 (2011)
59. H. Derakhshankhah, A.A. Saboury, R. Bazl, H.A. Tajmir-Riahi, M. Falahati, D. Ajloo, A.A. Moosavi-Movahedi, *J. Iran. Chem. Soc.* **9**(5), 737 (2012)

60. M. Saeidifar, H. Mansouri-Torshizi, Y. Palizdar, M. Eslami-Moghaddam, A. Divsalar, A.A. Saboury, *Acta Chim. Slov.* **61**(1), 126 (2014)
61. B.H.M. Hussein, *J. Lumin.* **131**(5), 900 (2011)
62. F. Samari, B. Hemmateenejad, M. Shamsipur, M. Rashidi, H. Samouei, *Inorg. Chem.* **51**(6), 3454 (2012)
63. T. Mukherjee, B. Sen, E. Zangrando, G. Hundal, B. Chattopadhyay, P. Chattopadhyay, *Inorg. Chim. Acta.* **406**, 176 (2013)
64. C. Qiao, S. Bi, Y. Sun, D. Song, H. Zhang, W. Zhou, *Spectrochim. Acta Part A Mol. Biomol. Spectrosc.* **70**(1), 136 (2008)
65. S. Kashanian, A.T. Ghobadi, *DNA Cell Biol.* **30**(12), 1085 (2011)
66. A.O.F.R. Supercomplexes, *J. Biol. Chem.* **289**(9), 6133 (2014)
67. G. Zhang, X. Hu, N. Zhao, W. Li, L. He, *Pestic. Biochem. Physiol.* **98**(2), 206 (2010)
68. M. Khorasani-Motlagh, M. Noroozifar, A. Moodi, S. Niroomand, *J. Photochem. Photobiol. B Biol.* **127**, 192 (2013)
69. H. Mansouri-Torshizi, S. Zareian-Jahromi, K. Abdi, M. Saeidifar, *J. Biomol. Struct. Dyn.* no. just-accepted, 1 (2018)
70. N. Raman, J.D. Raja, A. Sakthivel, *J. Chem. Sci.* **119**(4), 303 (2007)
71. I. Wiegand, K. Hilpert, R.E.W. Hancock, *Nat. Protoc.* **3**(2), 163 (2008)
72. V. Reddy, N. Patil, T. Reddy, S.D. Angadi, *J. Chem.* **5**(3), 529 (2008)
73. B.G. Tweedy, *Phytopathology* **55**, 910 (1964)
74. A. Sahraei, H. Kargar, M. Hakimi, M.N. Tahir, *J. Mol. Struct.* **1149**, 576 (2017)
75. K.R.S. Gowda, H.S. Bhojya Naik, B. Vinay Kumar, C.N. Sudhamani, H.V. Sudeep, T.R. Ravikumar Naik, G. Krishnamurthy, *Spectrochim. Acta Part A Mol. Biomol. Spectrosc.* **105**, 229 (2013)
76. J. Pusz, E. Ciszkowicz, K. Lecka-Szlachta, S. Wolowiec, E. Woznicka, *J. Acta Pol. Pharm.* **74**(4), 1101 (2017)